forests

MDPI

Article

Effects of an Invasive Bark Beetle *Polygraphus proximus* Blandf. Outbreak on Carbon Pool Dynamics in West Siberian Dark Coniferous Forests

Ivan A. Kerchev *, Elvina M. Bisirova, Nikita A. Smirnov, Igor G. Grachev, Artem N. Nikiforov and Daria A. Kalashnikova

Institute of Monitoring of Climatic and Ecological Systems, Siberian Branch of the Russian Academy of Sciences, Akademicheskiy pr. 10, 634055 Tomsk, Russia; bissirovaem@mail.ru (E.M.B.); niknov918@gmail.com (N.A.S.); grachevimces@gmail.com (I.G.G.); a.nik-n@mail.ru (A.N.N.); terrezaprk@mail.ru (D.A.K.)
* Correspondence: ivankerchev@gmail.com

Abstract: Invasions of dendrophagous insects pose major threats to forest ecosystems and to the timber industry. The alien species bark beetle *Polygraphus proximus* Blandf. of Far Eastern origin has caused Siberian fir dieback in vast areas within several regions of Russia. Rapid spread of the pest and its outbreaks raise the issue of preserving the most important functions, including carbon sequestration, by the damaged forests. In this study, monitoring of carbon pool dynamics was carried out during 2012–2023 on four sample plots showing various degrees of damage in the southern taiga zone of Western Siberia in the Larinsky Landscape Reserve. Dynamics of the forest stands' vitality were reflected in a rapid decline of the number of viable trees and an increase in amounts of deadwood, debris, and soil composition, resulting in a transformation of the natural biological carbon cycle in the native dark coniferous ecosystems.

Keywords: bark beetle; carbon; invasion; outbreak foci; Siberian fir; Western Siberia

Citation: Kerchev, I.A.; Bisirova, E.M.; Smirnov, N.A.; Grachev, I.G.; Nikiforov, A.N.; Kalashnikova, D.A. Effects of an Invasive Bark Beetle *Polygraphus proximus* Blandf. Outbreak on Carbon Pool Dynamics in West Siberian Dark Coniferous Forests. *Forests* **2024**, *15*, 542. https://doi.org/10.3390/f15030542

Academic Editor: Rastislav Jakuš

Received: 29 December 2023
Revised: 4 March 2024
Accepted: 14 March 2024
Published: 15 March 2024

1. Introduction

Worldwide, forests represent up to 80% of aboveground carbon (C) and ≈40% of underground C [1,2]. The preservation of C in forest ecosystems is imperative for mitigating C emissions and combating climate change [3]. Nonetheless, the risk of C emissions triggered by forest disturbances must be taken into account when C budgets are estimated [4].

In recent decades, the rate of forest C sequestration has slowly declined due to the increasing frequency and magnitude of disturbances (e.g., wildfire), leading to abrupt and/or gradual transfers of C to the atmosphere and to dead organic matter pools. Foresters and ecologists worldwide have been detecting the dieback of conifers across the boreal zone [5–9]. The ongoing deterioration of the condition of dark coniferous forests in Russia is influenced by the increasing frequency of extreme natural phenomena, mostly related to climate change (e.g., high temperatures, droughts, fires, and strong winds). Deterioration of the condition of forest stands is also due to aerotechnogenic impacts, unfavorable local climatic and soil conditions, the substantial age of forest stands, the spread of fungal and bacterial diseases, and outbreaks of insect pests [5,10–12].

The loss of forest stands resulting from natural processes is rapidly worsening due to another problem that has been widely recognized around the world, that is, alien pest invasions, which pose a serious threat to biodiversity and ecosystem functioning [13–15]. Over the past three decades, the presence of several alien species of dendrophages in Russia have led to considerable environmental and economic losses and resulted in negative social consequences [16].

One example of the consequences of the penetration of such alien species into new territories is the invasion by the four-eyed fir bark beetle *Polygraphus proximus* Blandf.

(Coleoptera: Curculionidae, Scolytinae), an endemic pest from the Far East. This has resulted in rapid drying out of the Siberian fir *Abies sibirica* Ledeb. in large areas, from the East European Plain to the south of Eastern Siberia, in only a few decades [17–20]. Despite the known possibility of development of the alien bark beetle on various representatives of the family Pinaceae in forests, it has been found almost exclusively on Siberian fir [21]. In forest stands, weakened trees are colonized first. At high abundance, these beetles cause the death of healthy fir trees in 2–3 years [21]. The rapid increase in the abundance of pests in forest stands is associated with the presence of two generations per season, the re-emergence of females, and sister brood establishment [21,22]. The preferred trees for *P. proximus* are those with a diameter of 9–22 cm but, at high abundance of the pest, large undergrowth is also colonized, and thicker trees are occupied together with the native white mottled sawyer *Monochamus urussovi* Fisch. [23].

The factors that have led to the rapid spread of the bark beetle in the region of invasion are the absence of effective mechanisms of resistance of Siberian fir to symbiotic ophiostomatoid fungi spread by this pest, favorable climatic conditions for the beetle in its new habitat, and the existence of vast territories dominated by fir [12,17,18,23,24].

Previously, it has been demonstrated that forest canopy transformations provoked by a *P. proximus* outbreak cause significant qualitative and quantitative changes in the biota, thus serving as an important factor in the latest zoogenic successions in dark coniferous ecosystems of the Siberian taiga [25]. The death of native dark coniferous forests caused by *P. proximus* (similar to cases presenting striking examples of extensive outbreaks of other aggressive dendrophages) is also accompanied with environmental risks associated with forest communities losing their most important functions, namely, water protection, environment formation, and carbon sequestration. In this context, an important and insufficiently studied issue is the quantitative assessment of the time course (dynamics) of these functions. Assessment of the levels of carbon sequestration capacity of stands before and after an alien pest outbreak and the rate of transition of carbon stored by wooden phytomass into dead organic matter (debris) are of particular note, as well as the response of soil mineral layers to these rapid ecosystem transformations.

The purpose of this study was to analyze the impact of an alien bark beetle on the condition of trees and carbon pool dynamics in woody phytomass and in soil by means of a case study of disturbed forest stands in the Larinsky Landscape Reserve during a 12-year period of monitoring.

2. Materials and Methods

2.1. Study Area

The study was conducted on four permanent sample plots established in the Larinsky Landscape Reserve, located at 56°12′43″ N, 85°02′20″ E, which has regional significance as part of Kolarovskiy District forestry within Tomsk forestry, Kolarovskoye stow. This reserve, with a total area of 1686 hectares, is located in the south of Tomsk Oblast, on the Tom-Yaya interfluve in the lower reaches of the Tugoyakovka River (the right tributary of the Tom River), and contains a reference section of a transition zone from the flat southern taiga to the mountain taiga of the Kuznetsk Alatau, with patches of indigenous dark coniferous forests dominated by *Abies sibirica* Ledeb. The maximum height is 180 m above sea level (Figure 1). The climate of the study area is continental cyclonic with long cold winters and short hot summers, and is transitional between the temperate continental Russian Plain and the sharp continental climate of Eastern Siberia. The average annual temperature is −0.9 °C and the frost-free period is 110–120 days. Winter is harsh and long. The average January temperature is −17.1 °C and the average July temperature is 18.7 °C. The annual precipitation is 568 mm and most of it falls within the warm period of the year.

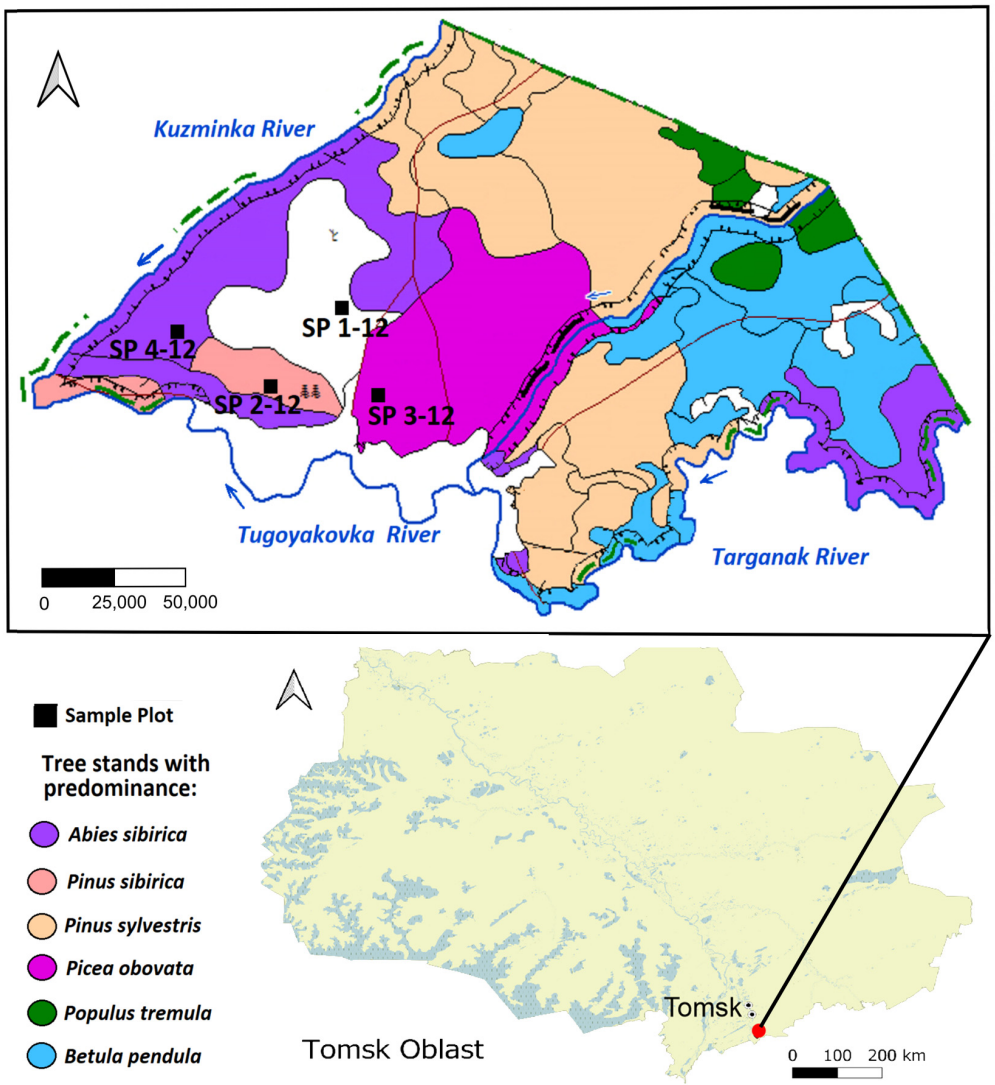

Figure 1. The map of survey sites in the study area.

Since the 1950s, the territory of the reserve has remained unaffected by the anthropogenic impact and stressors such as outbreaks of aboriginal pests, massive windfalls, and storm damage [25]. As a starting point for the state of the tree cover (when tracking the dynamics of its changes caused by the pest invasion), we used data from the inventory of forest stands that was carried out in the reserve before the development of the *P. proximus* outbreak. Dendrochronological analysis of the longest-dead (including fallen) trees in this stand with characteristic signs of *P. proximus* infestation had previously shown that the drying out caused by the alien bark beetle in this stand began no later than 2005 [26]. Considering that all areas were located at a distance an order of magnitude less than the dispersal flight range of *P. proximus*, they can be attributed to one outbreak focus and one population of the pest [21,25].

In 2012, in the parts of the reserve with various magnitudes of the disturbance caused by the *P. proximus* outbreak, permanent sample plots of 0.15–0.25 ha were established that contained at least 100 dominant trees in the main canopy, for which stand inventory was carried out (diameter at breast height [DBH], height, age, completeness, and quality class). Tree-by-tree surveys were repeated in the years 2018 and 2023. The inventory characteristics of the analyzed tree stands, according to the latest survey (in 2023), are given in Table 1.

Table 1. Inventory data of stands in the sample plots.

No. of Sample Plot	Sample Area, ha	Stand Composition *	Total Number of Trees, pcs/ha	Number of Living Trees, pcs/ha	Live Stand Volume, m^3/ha	Total Stand Volume, m^3/ha	Average Age, Year	Average Diameter, cm	Average Height, m	Quality Class	Stand Density
1-12	0.2	Dead forest stand:								II	
		75F **	485	25	4	372	94	28.6 ± 0.9	24.1 ± 0.9		0.007
		13SP	25	5	3	78	160	59.0 ± 12.3	25.0 ± 0.4		0.004
		11S	30	20	15	35	120	49.3 ± 8.1	24.0 ± 1.9		0.04
		1P	10	10	5	5		25.5 ± 1.6	20.8 ± 0.9		
		Single trees ***:									
		76S	20	20	4	4		47.6 ± 9.1	23.4 ± 2.1		
		9F	25	25	3	3		18.4 ± 1.2	16.2 ± 0.4		
		9P	10	10	15	15		25.5 ± 1.6	20.8 ± 0.9		
		6SP	5	5	5	5		28	24		
		2 layer:									
		98F	655	655	38	38		11.0 ± 0.3	8.4 ± 0.3		0.28
		2S	15	15	0.6	0.6		10.9 ± 1.6	9.2 ± 1.7		
2-12	0.25	$53F_1$	308	172	126	229	68	28.9 ± 1.3	21.9 ± 0.5	II	0.34
		$5F_2$	456	200	12	26		14.3 ± 0.5	13.1 ± 0.5		0.07
		22SP	56	24	53	142	150	47.0 ± 4.2	23.0 ± 1.2		0.09
		18S	44	36	42	43		33.3 ± 4.1	23.3 ± 1.8		0.10
		2B	12	12	5	5	35	18.1 ± 7.4	13.6 ± 3.1		0.03
3-12	0.25	$53S_1$	112	84	124	149	107	38.7 ± 4.9	24.6 ± 0.9	II	0.12
		26SP	32	28	61	65	133	44.2 ± 3.9	23.9 ± 0.9		0.10
		$11F_1$	140	32	35	112	106	34.9 ± 3.1	22.9 ± 1.3		0.09
		7P	20	16	18	19	120	37.1 ± 2.4	24.8 ± 0.4		0.05
		$2F_2$	212	84	4	16	65	9.4 ± 0.6	9.4 ± 0.6		0.03
		$1S_2$	20	20	1	1	63	10.1 ± 1.1	10.0 ± 1.4		0.01
4-12	0.16	54SP	13	13	112	112	175	98.5 ± 1.5	27.5 ± 0.1	II	0.16
		$26F_1$	350	88	51	283	108	27.3 ± 2.1	20.1 ± 0.9		0.15
		15S	37	31	31	43		39.0 ± 2.8	24.2 ± 0.6		0.08
		$5F_2$	524	231	10	38	53	10.6 ± 0.5	8.4 ± 0.4		0.04
The arithmetic mean values ± standard error of the arithmetic mean is given											

* The share of participation of each tree species in the total volume of the forest stand (%). ** F: *Abies sibirica* Ledeb., SP: *Pinus sibirica* Du Tour, S: *Picea obovata* Ledeb., P: *Pinus sylvestris* L., B: *Betula pendula* Roth., F_1 and F_2: the first and second generation of fir, S_1 and S_2: the first and second generation of spruce. *** Composition of a sparse stand.

Investigating the influence of a pest on forest ecosystems first involves assessing the vitality of trees to determine the degree of degradation of forest stands at the time of the survey and identifying dynamics and environmental consequences of the invasion. For this purpose, in the sample plots, each tree with a diameter of 6.1 cm or more was labeled with a number, which allowed us to track their condition over a long period during the monitoring surveys.

Each tree in a forest stand was assessed according to a set of visual characteristics, using a scale of vitality categories that was created taking into account the relationship between the alien pest and its host tree species [25]. During the assessment of the tree condition by means of this scale, equivalent weights were given to specific features of the tree crown, the trunk, and internal features. The final evaluation of a tree's state was determined according to the worst grade (in a category) recorded in at least one of the groups of features.

The comprehensive assessment of the condition of forest stands on the sample plots was conducted through determining the proportion (%) of trees belonging to various vitality categories. This calculation was based on the cross-sectional area of trunks at breast height (1.3 m) for each category. Within a forest stand, the proportion of trees in a certain state was calculated on the basis of the following: the simplest calculation method by means of the number of trunks was considered unreliable [27]; the technique based on the volume of trunks was more accurate but required more effort. As a compromise, the method of areas of cross-sections was used; this is related to the volume of trunks [27,28].

Vitality category I corresponds to healthy trees, II to weakened trees, and III to heavily weakened trees. Trees in categories I, II, and III are viable (maintaining the basic functions of living trees), those in category IV are dying, category V comprises trees that died in the current year (recent dead trees), and category VI comprises trees that died in previous years (long-dead trees). Detailed descriptions of the characteristics of each category are given in Appendix A. To show the speed of accumulation of windfall trees and storm-damaged trees in forest stands damaged by the pest in question during the observation period, category VII was introduced: "fallen trees".

2.2. Evaluation of Dynamics of the Wood Phytomass Pool

Core samples from representative trees were taken from at least 10% of all trees on each sample plot using a Pressler incremental drill [29]. Dendrochronological analysis (radial growth, the total radius and diameter of the trunk excluding bark, and the percentage ratio of radial growth to the total radius) was performed on LINTAB 6 in TSAP-Win Professional 4.64 software.

The phytomass of forest stands was calculated via an allometric model designed to assess carbon reserves and annual carbon sequestration according to V.A. Usol'tsev [30]:

$$\ln P_i = a_0 + a_1 \ln H + a_2 \ln DBH \quad (1)$$

where P_i is the phytomass in the absolutely dry state of trunks (with bark), of the branch skeleton, of needles (foliage), of aerial parts, and of roots (P_{st}, P_{br}, P_f, P_a, and P_r, respectively), kg; H is tree height, m; DBH is trunk diameter at breast height, cm; a_0, a_1, and a_2 are regression coefficients calculated from empirical data for forests of Northern Eurasia through taking into account the species affiliation, age, and growth conditions of tree species [30,31].

Assessment of phytomass stocks in each fraction (trunk, skeleton of branches, needles/foliage, and roots) of trees was performed on 696 trees in the 2012–2023 period. Determination of the carbon content of the main forest-forming species was performed on 113 samples of the wood fractions under study: the trunk, branches, roots, and leaves/needles.

2.3. Debris Stock Assessment

The survey of large woody debris was carried out only in 2023 on eight survey plots (two per sample plot) measuring 10 × 10 m. During the setup, survey plots were chosen so

that they were at least 15 m away from edges of a sample plot and so that the distribution of debris on a survey plot was uniform.

When the wooden mortmass was registered, all above-ground woody remains (stumps and dead standing trees) and fallen woody remains with a diameter of 4 cm or more were recorded. For all samples of debris, the following were registered: species, DBH for dead standing trees, and two diameters for fallen trees (any part of the woody debris that was outside the perimeter line was ignored); for stumps: the diameter at the root neck and at the top; for dead standing trees and stumps: height, length of fallen trunks and branches, and degrees of decomposition [32,33]. The volume of stumps and fallen trees was calculated using the truncated-cone formula. Volumes of large woody debris were summed up by species and by decomposition degree. The degree of decomposition from 1 to 5 was determined by means of several external signs such as decrease in wood density, the presence and degree of decomposition due to saprotrophic organisms, humification, and colonization by mosses, lichens, and higher plants of the ground cover [34].

The density of samples at various degrees of decomposition was determined through measurement of the buoyancy force of the samples immersed in water [33].

2.4. Soil Analysis

Soil analysis was carried out using soil sections. Surface litter was collected separately. Mineral samples were collected from the front wall of a soil profile, in a continuous column at every 5 cm, taking into consideration the spatial variation of genetic horizons. All samples were placed in plastic bags. To quantify the moisture content under natural conditions and to calculate soil density, additional sampling of mineral horizons was performed by means of a cutting ring (to obtain a core sample 4 cm high and 4 cm in diameter) [35,36]. In total, 9 soil sections were designated in the study area, and more than 150 organogenic and mineral samples were taken from them to determine the general properties, reserves of nutrients, and root density. In addition, samples from the sample plots were collected in triplicate using a soil drill within a continuous column at 10 cm intervals to a depth of 200 cm. The samples were transported to the laboratory, where they were homogenized: all visible mineral components (soil lumps and stones) were removed from organogenic samples, and the roots were removed from mineral samples. All samples were air-dried and stored in plastic bags. The soil section of sample plot SP 3 was excluded from the analysis because the site is located on a slope, and also owing to signs of turbation processes in the soil profile.

2.5. Sample Preparation and Chemical Analysis of the Wood and Soil Samples

The preparation of wood samples for carbon quantitation was as follows: first, the wood samples were dried at room temperature for 24 h, and then they were ground in a laboratory mill. Each ground sample was passed through a sieve (less than 1.2 mm) to eliminate large sawdust, and then passed through the mill and the sieve again. This process was repeated 2–3 times to obtain sawdust of uniform size, after which the homogenized sawdust was dried at 60 °C for 24 h, placed in a labeled paper bag, and subjected to analysis.

The total carbon content of wood samples was determined via elemental analysis coupled with isotope ratio mass spectrometry [37] on a DELTA V Advantage isotope ratio mass spectrometer combined with a Flash 2000 elemental analyzer (Thermo Fisher Scientific, Bremen, Germany). Measurement of the percentage content of total carbon was based on instantaneous combustion of a sample (weighing ≈ 0.450–0.500 μg) in an oxidation–reduction reactor. Samples packed into tin capsules were burned at 1020 °C in a flow of a carrier gas (high-purity helium, purity of at least 99.9999%, at 250 mL/min) with simultaneously supplied pure oxygen (at 180 mL/min). The obtained CO_2 in the helium flow passed along the capillary into the DELTA V Advantage mass spectrometer through a Conflo IV gas-distributing system. Before the start of the analysis, three to five measurements of standards [IAEA-600 (caffeine), IAEA-CH-3 (cellulose), and EMA

P2 (certified reference material)] were carried out. The standard deviation of the carbon percentage measurements did not exceed 0.1%.

Percentage contents of total nitrogen and total carbon in soil samples were determined on an EMA 502 elemental CHNS-O analyzer (VELP Scientifica, Usmate (MB), Italy). Samples were burned at 1030 °C in a combustion chamber to obtain elemental inorganic compounds. After the combustion, the gases in the carrier gas flow (high-purity helium, purity of at least 99.9999%) entered the column where the components were separated. Quantitative analysis of the elements present in the gas mixture was performed using a thermal conductivity detector. The measurement error was no more than 0.2%. To analyze soil samples, a preset "Soil method" [38] with the following parameters was employed: gas chromatographer oven temperature, 55 °C; minimum volume of O_2, 10 mL; MFC_1 and MFC_2 He flow rates, 120 and 140 mL/min, respectively; O_2 flow rate, 300 mL/min; O_2 factor, 0.7 mL/mg; weight of a sample, 10–20 mg.

2.6. Statistical Analysis

Basic descriptive statistics of the study sample (e.g., the mean of a characteristic, error, and variance) were obtained using Microsoft Excel 2016. In the STATISTICA 10 software package, the normality of the distribution of data was tested using the Shapiro–Wilk and Kolmogorov–Smirnov tests. The distribution was not normal in most cases, and therefore nonparametric methods were chosen for the data processing. For calculating a correlation between parameters of debris, Spearman's coefficient was used. Comparisons of wood phytomass between the initial, transitional, and final stages of stands were made using Friedman ANOVA and the Kendall coefficient of concordance. In all the statistical analyses, the significance level (p) was set to 0.05.

3. Results and Discussion

3.1. The Time Course of Vitality of Forest Stands

Since the last inventory in the surveyed stands, significant changes have been noted in the wood stock of growing Siberian fir trees (χ^2 (N = 4, df = 3) = 8.38, p = 0.04), due to the avalanche-like rate of their death caused by *P. proximus* (Figure 2).

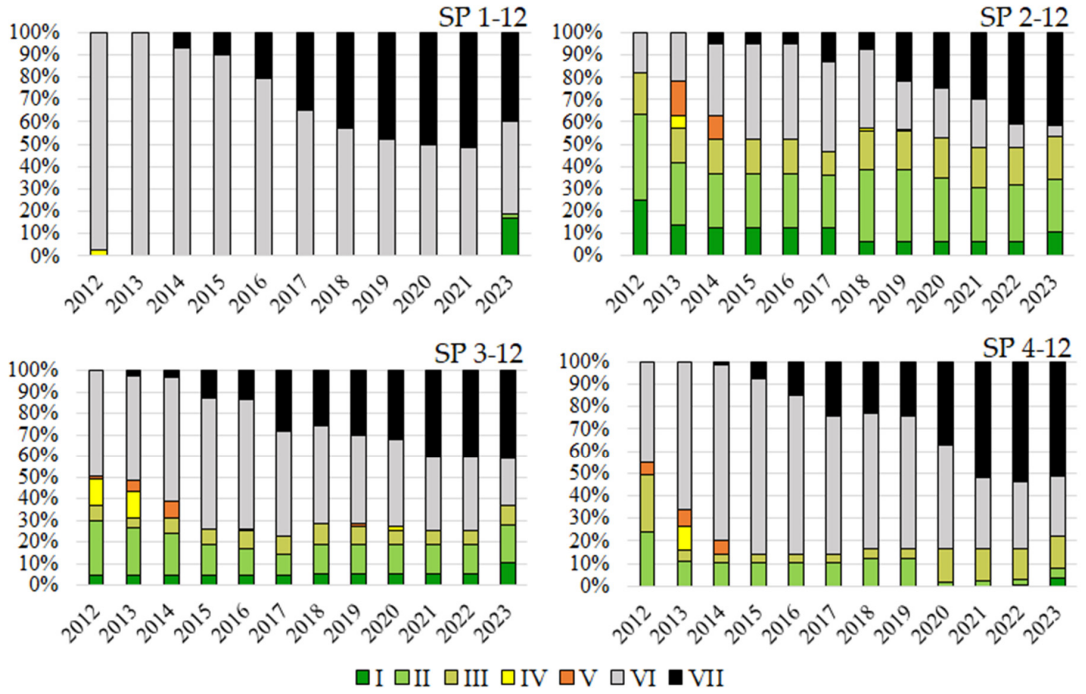

Figure 2. Vitality spectra of the studied fir stands (I: healthy trees, II: weakened trees, III: heavily weakened trees, IV: dying trees, V: recent dead trees, VI: long-dead trees, and VII: fallen trees).

Nonetheless, despite the consistency of changes in vitality between forest stands (Kendall coefficient of concordance = 0.7), the level of tree mortality by 2012 varied widely between sample plots from mild to complete death of fir trees. In a completely degraded forest stand (sample plot SP 1-12), 99.8% of standing trees were dying or dead at the time of the survey in 2012.

Apparently, the initial outbreak focus of the bark beetle in the reserve emerged precisely at this point. Here, throughout the entire observation period, only active accumulation of fallen trees was noted: from 7% in 2014 to 51.6% in 2021.

High degradation at the time of the initial analysis was also noted in fir stands of different ages on sample plots SP 3-12 and SP 4-12. Here, trees of the second generation were more damaged than those of the first. Well-pronounced weakening of fir trees was also observed in a forest stand on SP 2-12, which is the youngest of all surveyed plots (Table 1).

Analysis of data on the state of trees in forest stands showed that relevant processes in the investigated forest stands developed according to similar scenarios. Even at the beginning of this study in 2012, an unsatisfactory condition of forest stands was detected due to massive death of trees in previous years under the action of *P. proximus*. During further observation, there was only a worsening of the negative trends, as evidenced by an increase in the proportion of weakened, heavily weakened, and dead trees, as well as a massive accumulation of fallen trees in the preceding years, mainly owing to the breaking and falling of dead standing trees.

The peak of mortality (the sum of dying trees and recent dead standing trees at a given time point) occurred in 2013 on all sample plots (Figure 2). The rapid rate of death of fir trees during this period is explained by a substantial increase in air temperature in the summer of 2011 and the dry and hot weather in 2012, which had a negative influence on the physiological state of the trees and helped to increase the abundance and harmfulness of *P. proximus* [12].

The fastest rates of degradation during the observation period were identified in the years 2012–2014; next, massive accumulation of fallen trees was noted, and in some years, drying out of only a few trees was observed. Recent dead wood initially accumulated from a cohort of weakened small trees that were the first to die as a result of bark beetle colonization. A similar pattern in the development of foci has also been noted in stands of *Abies veitchii* Lindl. (1861) for *P. proximus* in Japan [39]. As a rule, a gradual decline in stem pest outbreaks is mediated by depletion of the food supply (in the outbreak foci) consisting of susceptible trees and unfavorable weather conditions [12,40].

Successional dynamics on the studied plots led either to complete degradation of a maternal canopy (SP 1-12), where open space emerged, or to severe thinning of a forest stand (SP 2-12 and SP 4-12). The best preservation of the forest environment was observed in mixed forest stands owing to the participation of other tree species (SP 3-12). As previously shown, outbreak foci of this pest develop most rapidly in monospecies tree stands, and the rate of fir die-off is inversely proportional to the share of the accompanying tree species [23]. Here, despite the predominance of dead standing fir trees in the vitality spectrum, the preservation of the forest ecosystem was ensured by viable trees of cohabitating species.

Nonetheless, on all analyzed plots, by the year 2023, a change in the vitality profile was observed (i.e., a slight increase in the proportion of viable fir trees); this can be explained by processes of restoration of the damaged forests through undergrowth of advance regeneration. For instance, in the dead forest stand on plot SP 1-12, processes of restoration of fir trees by young stock were noted; these accounted for ≈18% of the total fir stock on the sample plots (Tables 1 and 2, Figure 2).

Due to the rapid rate of degradation of forest stands under the influence of *P. proximus* and to the accumulation of a large number of dead standing and fallen trees in the stands, there was a qualitative transition of the carbon sequestration function from a live component of ecosystems to a dead one.

Table 2. Dynamics of some inventory parameters of forest stands.

Year of Research	No. of SP	Stand Composition	Stand Density	Stand Volume, m^3/ha	Total Number of Trees, pcs/ha
Before invasion	1-12	75F13SP11S1P *	1.1	490	540
	2-12	59F32SP8S1B	1.0	426	752
	3-12	45S34$F_1$5$F_2$10SP5P	1.0	300	412
	4-12	57$F_1$6$F_2$20SP14S3AS	1.0	506	760
2012	1-12	Single trees ** 52SP44S3P1F	0.2	123	75
	2-12	42SP47F10S1B	0.8	333	444
	3-12	52S25$F_1$14SP8P1F_2	0.5	219	228
	4-12	35SP44$F_1$20S1F_2	0.6	291	259
2018	1-12	Single trees ** 52SP44S3P1F	0.2	123	75
	2-12	45SP42F12S1B	0.7	334	412
	3-12	54S20$F_1$15SP10P1F_2	0.5	199	180
	4-12	55SP25S19F_1 1F	0.5	251	153

* F: *Abies sibirica* Ledeb., SP: *Pinus sibirica* Du Tour, S: *Picea obovata* Ledeb., P: *Pinus sylvestris* L., B: *Betula pendula* Roth., AS: *Populus tremula* L., F_1 and F_2: the first and second generation of fir. ** Composition of a sparse stand.

3.2. Dynamics of the Woody Phytomass Pool

On the sample plots, *S. caprea* is extremely rare in the species profile (two trees on two sample plots with a total weight of 460.1 kg); therefore, according to the IPCC guidelines [41], the carbon content of living wood was calculated and found to be 50%. For other species, it was empirically found that the C content varies from 47.41% for birch to 51.47% for Siberian pine. Upon examination of wood fractions, the C content proved to be the lowest in the needles of Scots pine (42.54%), whereas the highest C content was detected in branches of Siberian pine (53.46%) (Appendix B). Our data indicate a higher C content (by an average of 1%) in dark coniferous species compared to deciduous species, in agreement with results reported in the literature [42].

After a comparison of the results of allometric modeling to the elemental carbon content of the analyzed wood fractions from the several species under study, a quantitative estimate of the reserves of carbon was obtained. Throughout the entire study period, the total reserves of carbon sequestered by forest stands increased by 5.45% or 18.91 t/ha (Figure 3).

The increase in carbon reserves on the plots was implemented mainly by Siberian pine and fir, whose proportion of the total amount of carbon deposited in forest stands in the year 2023 was 85.87%.

Despite the increase in deposited carbon within forest stands, the phytomass of viable trees (vitality categories: I–III) was decreasing overall from 373.56 t/ha in 2012 to 337.79 t/ha in 2023. The dynamics of the proportion of viable trees differed among sample plots. For plot SP 1-12, where viable trees in 2012 constituted only 22.25%, their proportion diminished to 16.79% in 2018, owing to the death of mainly Siberian pine and spruce. Despite the transition of fir undergrowth into the main layer in the 2018–2023 period, the proportion of viable trees is currently only 18.26%. SP 2-12 is characterized by a gradual reduction in the proportion of trees in vitality categories I–III from 83.11% in 2012 to 61.63% in 2023. The main losses in tree stand phytomass affected Siberian pine and fir: Siberian-pine phytomass in the year 2012 decreased by 64%. In spruce–fir stands on SP 3-12, between the years 2012 and 2018, a gradual decline in the proportion of viable trees was detected, i.e., from 77.8% to 62.12%. These dynamics are due to the death of fir stands and partly due to recent spruce deadwood. In this area of the forest, an outbreak of the fungus *Heterobasidion annosum* (Fr.) Bref. was identified; this causes destructive rot of the root system, which led to a partial fall of spruce under the conditions of a slope. Nevertheless, on this sample plot, we registered an increase in the ratio of live phytomass of forest stands

to mortmass of dead standing trees because of the preservation and increase (since 2019) of the phytomass of mainly spruce and Siberian pine owing to the growth of trees as well as the emergence of undergrowth into the main layer. On SP 4-12, there was a gradual decrease in the proportion of viable trees from the year 2012 (51.85%) to 2018 (38.78%), owing to the death of fir; phytomass diminished by 63%. Since 2018, however, because of the emergence of fir undergrowth into the main layer and the growth of Siberian pine, the proportion of viable trees increased by 8.27%.

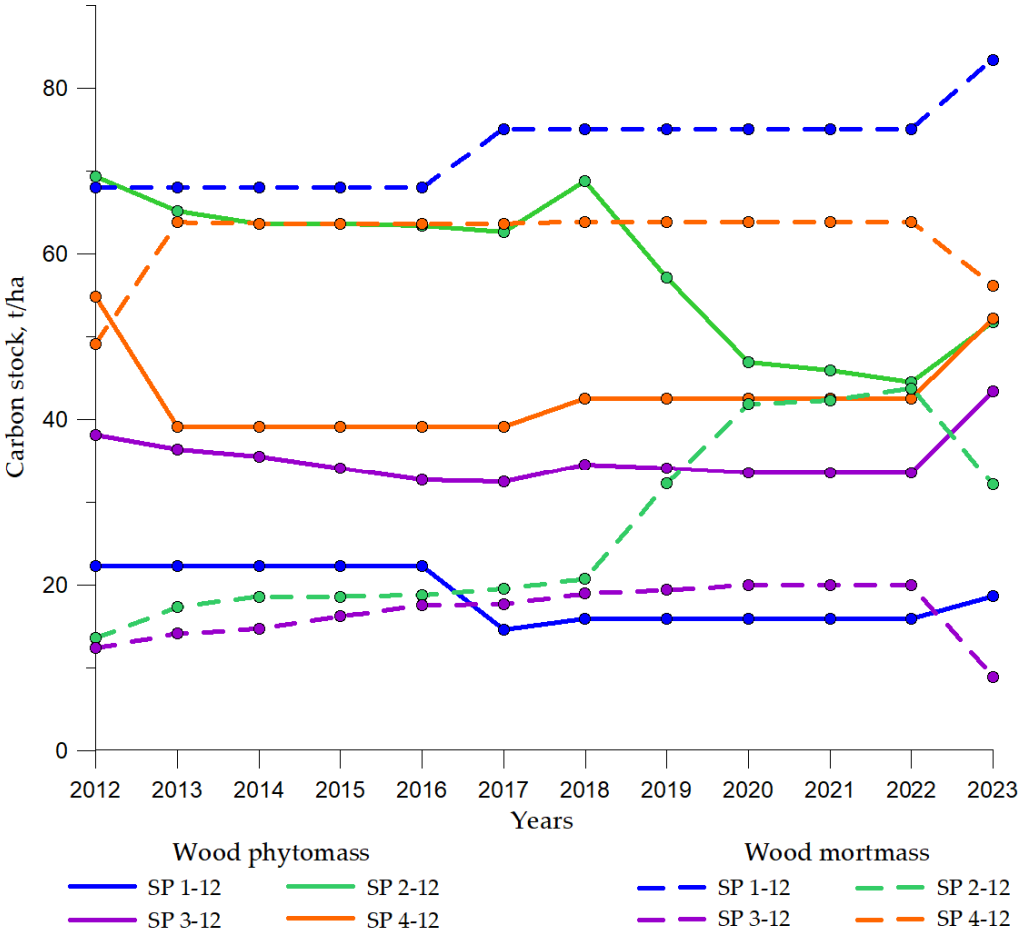

Figure 3. The time course of carbon in wood phytomass and mortmass on the sample plots under study.

A decrease in the vitality of trees in a forest stand directly causes a reduction in the carbon accumulation function of forest communities. In addition, the negative dynamics of sequestration potential among the species present in the forest stands in question were associated primarily with the death of Siberian fir as a consequence of damage by *P. proximus* and with the mass death of Siberian pine (observed in the past few years) under the action of another invasive bark beetle, i.e., the small spruce bark beetle *Ips amitinus* Eichh. (Coleoptera: Curculionidae, Scolytinae) [43]. For instance, the phytomass of viable fir diminished by 42.11 t/ha from 2012 to 2018. Nonetheless, due to the transition of some young trees into the main canopy, by the year 2023, phytomass indicators of live fir trees reached the values of 2012. For Siberian pine, there was a rapid reduction in phytomass having sequestration ability. According to our findings, despite the increase in deposited carbon reserves due to annual growth, the proportion of viable Siberian pine trees decreased by 29.29%, i.e., in phytomass equivalents, from 154.34 t/ha in 2012 to 109.13 t/ha in 2023.

Throughout the entire observation period, there was an increase in the phytomass of viable spruce trees from 71.81 to 75.17 t/ha. Positive dynamics of phytomass were also documented for birch, willow, and Scots pine. As studies on North American hemlock stands show, damage by aggressive dendrophages induces alterations in successions, in which, after the death of a coniferous species, there is gradual replacement with deciduous trees that have a higher rate of C sequestration [44]. In this context, it is necessary to take into account that a change in species composition of the forest stands we examined is being hampered by the initially low number of deciduous species in the maternal canopy, by rapid overgrowth of disturbed areas with tall grasses, and by the presence of abundant undergrowth of Siberian fir of advance regeneration.

3.3. Estimation of Carbon Reserve Contents of Debris

The carbon content of whole-wood samples of Siberian-fir debris ranged from 44.20 to 52.27%, with an average value of 47.04% (±2.20%; Table 3).

Table 3. The total carbon content (C, %) of whole-wood samples of *Abies sibirica* at different decomposition degrees.

Decomposition Degree	C, %		
	Min	Max	Mean ± SD
1st	45.68	46.65	46.30 ± 0.54
2nd	44.85	46.08	45.51 ± 0.45
3rd	45.63	49.83	47.63 ± 1.67
4th	44.41	52.00	47.36 ± 2.75
5th	44.20	52.27	47.72 ± 3.02
all samples (n = 35)	44.20	52.27	47.04 ± 2.20

For the 1st and 2nd decomposition degrees, the percentage content of carbon was 45.75% ± 0.60% (mean ± SD). For the 3rd–5th decomposition degrees, the percentage content of carbon was high: 47.56% ± 2.40%. Overall, the C levels in whole-wood samples of fir are consistent with the literature data on *Picea abies* Karst. in Finland and *Picea mariana* Britton, Sterns, and Poggenb in Canada [45,46].

As a result of empirical measurements, an inverse correlation with the degree of decomposition was revealed for the density of fir wood ($r_s = -0.74$, $p \leq 0.5$), as was a very high positive correlation with its carbon content ($r_s = 0.94$, $p \leq 0.5$) (Figure 4).

At the first degree of decomposition, the density was 412.8 ± 37.26 kg/m^3 and gradually decreased by almost 76%, reaching 234.8 ± 60.5 kg/m^3 at the fifth degree of xylolysis, in agreement with the literature data regarding a physicochemical analysis of decomposing wood [33].

According to our measurements, the percentage content of carbon (by weight) in live stem wood of Siberian fir is 46.8%. Thus, as a consequence of heterotrophic decomposition, from degree 1 to 5, fir wood loses ~70% of its carbon.

Dark coniferous fir forest stands are characterized by high values of deadwood stocks, ranging from 208 to 463 m^3/ha, which exceed live wood stocks by 1.2–6.8-fold (Table 4).

Table 4. Stocks of live and dead wood in dark coniferous fir forest stands on the surveyed sample plots.

SP	Living Trees, m^3/ha	Stocks of Debris, m^3/ha	Carbon in the Debris, t/ha	Weighted Average Category of Stand Vitality
1-12	65.6	445.38	51.4	4.5
2-12	238	438.39	60.5	2.7
3-12	243	208.11	23	2.8
4-12	204	463.58	60.2	3.8

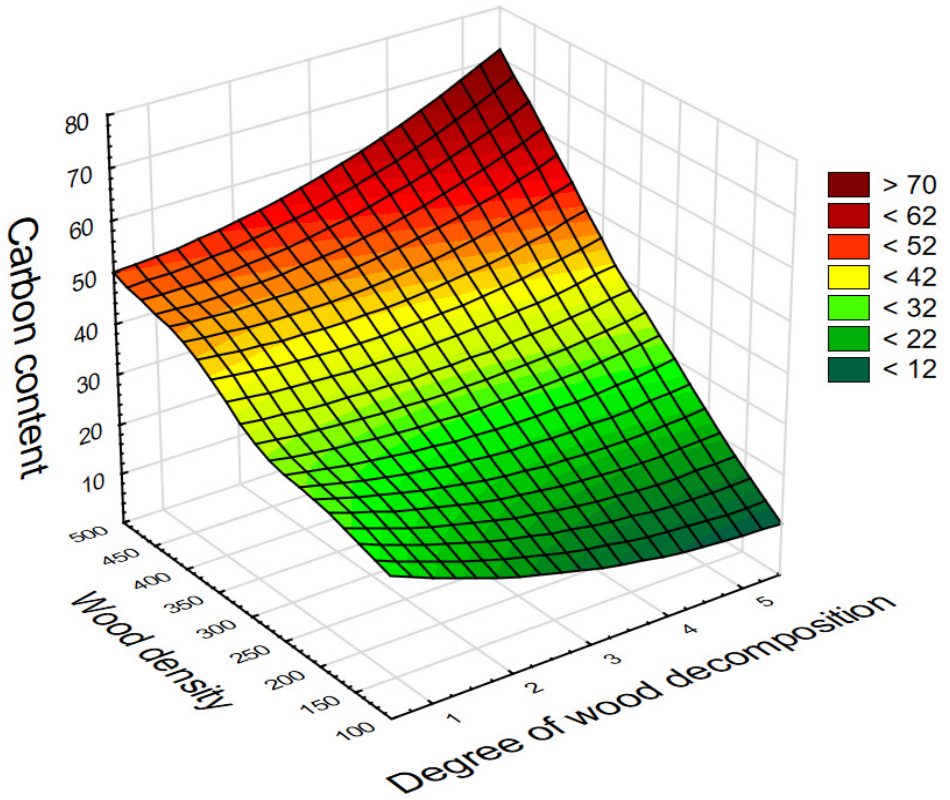

Figure 4. Correlations of the carbon content and of *Abies sibirica* Ledeb. wood density with the degree of decomposition.

Furthermore, according to our analysis taking into account the degree of decomposition, a species ratio, and the results of chemical analysis of deadwood, the level of carbon in forest stands varies between 23 and 60.5 t/ha.

The main stocks of large woody remain (75–100%) on all four surveyed plots have been formed by Siberian fir, with the exception of plot SP 1, where there is a minor admixture of *P. sibirica*, *Picea obovata* Turcz., *Populus tremula* L., *Sorbus sibirica* Krylov, and *S. caprea*. In the examined forest stand on SP 3-12, Siberian spruce represents 9% of debris; on SP 4, aspen and Siberian pine constitute 18% and 7%, respectively.

Stocks of fir debris by degrees of decomposition on all sample plots were found to be distributed unevenly. The largest amount of woody remains corresponded to the second and third degrees (42.68% and 30.21%, respectively); these remains formed mostly during the peak of the mass reproduction outbreak of the pest. The fourth and fifth degrees were represented by trees that died during the phase of pest abundance growth and by trees that died of other natural causes (16.21% and 10.63%, respectively). The smallest amount of fresh debris at the first degree of decomposition (0.27%) indicates a sharp slowdown of processes of fir death in forest stands because of the depletion of the food supply most suitable for the pest.

A study on the time course of stocks of large woody debris in fir forests damaged by the bark beetle *P. proximus* in Krasnoyarsk Krai shows that there is a sharp increase in the accumulation of debris with an increase in the degree of damage to fir stands [32]. The total reserves of debris in the Krasnoyarsk foci range from 73 to 195 t/ha; this is comparable to the reserves of debris in the Larinsky Landscape Reserve, which amount to 62–160 t/ha.

Similar indicators of debris accumulation have been shown in association with degradation processes in boreal forest stands observed during outbreaks of other aggressive dendrophages; for example, in outbreak foci of a phyllophage native to Siberian dark coniferous forests, i.e., the Siberian moth *Dendrolimus sibiricus* Tscetv. (Lepidoptera: Lasiocampidae). In Krasnoyarsk Krai, in a post-outbreak period, debris stocks in damaged

Siberian-pine stands reached 200–400 m^3/ha [47]. In the United States, a similar picture has been observed in outbreak foci of the mountain pine beetle *Dendroctonus ponderosae* Hopk. (Coleoptera: Curculionidae, Scolytinae) [48] and in outbreak foci of other forest pests, among which most are invasive species [49].

In dark coniferous forests that do not have a pronounced zoogenic load, the main factors of debris accumulation are the age of a tree stand, quality class, and the main forest-forming species, in which, in the absence of large fires, considerable accumulation of deadwood takes place. The latter parameter that we determined is more than 10 times higher than the average value for Russian forests: 32.2 m^3 debris/ha [50]. In addition, for middle-taiga dark coniferous forests of Siberia, the volume of accumulated deadwood according to the literature data averages 48–62 t/ha [51], which is comparable with our findings.

3.4. Soil

On the analyzed sample plots, qualitative and quantitative transformations of the soil profile occurred over 6 years. The change in some horizons was due to the transformation of organic residues and to intensification of their humification. Under conditions of biocoenosis alteration, as ground litter horizons degraded, they first increased their thickness by 2–4-fold, and then their lower part acquired the properties of humus. Thus, a shift in the boundaries of mineral horizons was observed. As a consequence, more potent humus-accumulating horizons formed, next giving way to transitional humus-eluvial horizons. The mineral strata below almost did not transform, but the mass and boundaries of the horizons changed.

The levels of soil carbon and nitrogen, similar to their distribution in the soil profile, underwent changes, especially in the upper 30–40 cm layer. In the forest stand at SP 4-12, the differences in soil carbon content were small and amounted to less than 1% in mineral and organic horizons. In the forest stand (SP 2–12), there was an increase in the amplitude of the divergence of values (up to 1%–2%) in the upper horizons of the profile. At the stage of complete degradation, collapse of the tree layer, and transformation of the biogeocenosis (SP 1-12), the amplitude of the discrepancy in the values of carbon content in mineral horizons reached 4% (Figure 5).

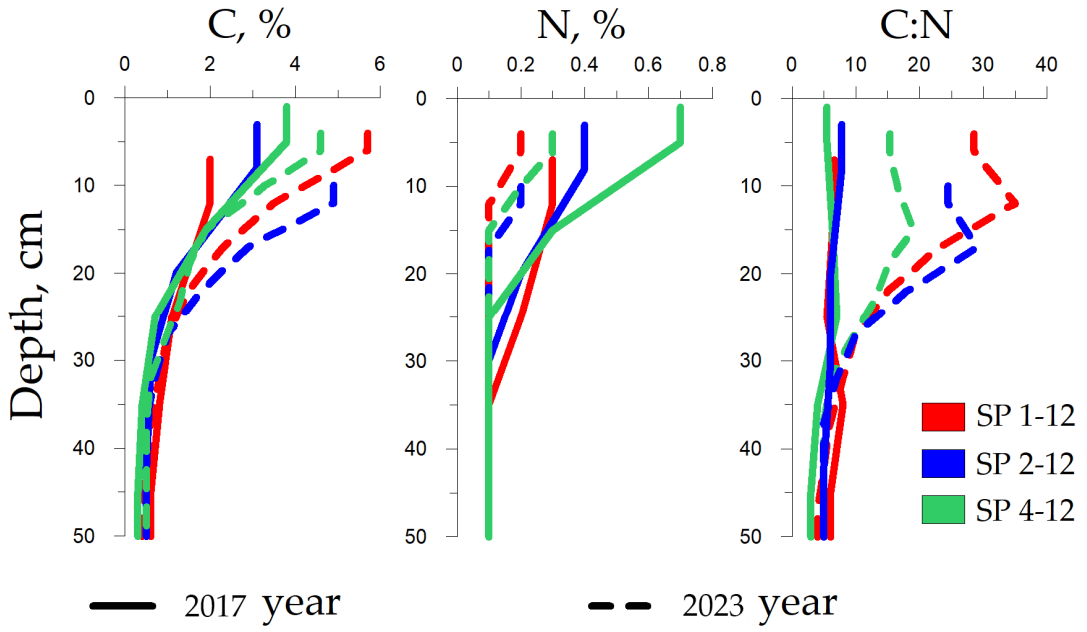

Figure 5. The distribution of carbon, nitrogen, and their ratio within the soil profile during the period from 2017 to 2023.

In addition, the nitrogen content at the beginning and end of the study diminished by an average of 2-fold, and the C/N ratio rose substantially.

Soil carbon reserves in the mortmass and mineral horizons of soils (down to a depth of 50 cm) varied considerably both among the degradation degree of the fir component of the forest and within the time series of observations (Figure 6). For instance, in the less damaged forest stand (SP 2-12), carbon reserves in ground litter horizons were slightly higher than in the soil; however, even at the stage of greater weakening of the tree layer (SP 4-12), there was a slight increase in the carbon reserves of the mineral horizons of soils. At the stage of complete death and decay of the forest stand (SP 1-12), the highest carbon reserves were confined to ground litter horizons because of the accumulation (on the soil surface) of mortmass of both soil cover and of deadwood.

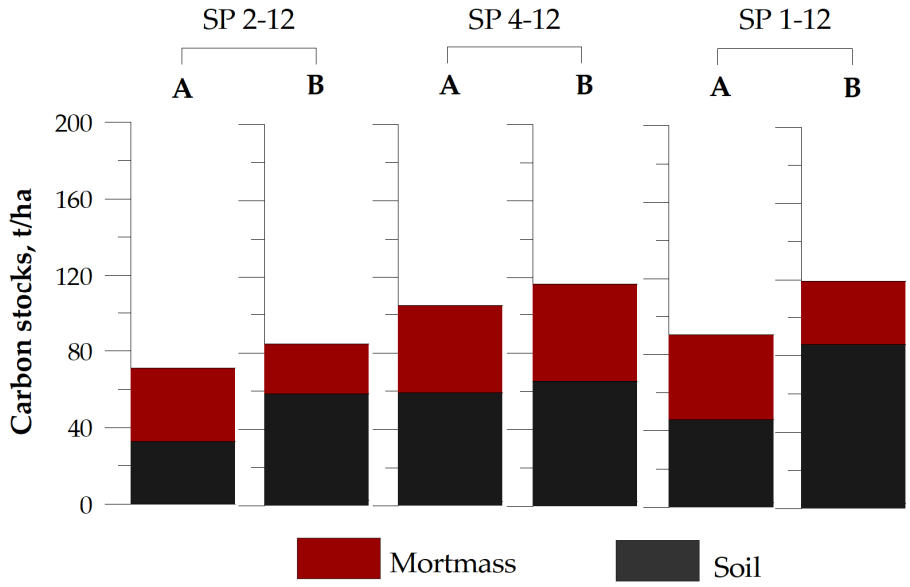

Figure 6. Carbon reserves in mortmass and in mineral horizons of the soil profile (for a layer of 0–50 cm) at the less damaged (SP 2-12), at the stage of medium degradation (SP 4-12), and at the stage of severe degradation (SP 1-12) for time points A (2017) and B (2023).

When assessing carbon reserves in the time series, it is evident that during the observation period (Figure 6), a decrease in carbon reserves was detected in mortmass, with a slight increase within mineral horizons.

As reported previously, the death of fir trees in forest stands as a result of constant damage by *P. proximus* induces microenvironment alterations, such as an increase in illumination and soil surface temperature and a qualitative change in soil cover [12]. Such shifts in microclimatic parameters can lead to a whole cascade in ecosystem processes, such as an increase in the rate of decomposition, higher availability and velocity of nutrient cycling, and lowered soil respiration [52–55].

Our examination of the pattern of distribution of several elements, including biogenic elements (C and N), points to a re-distribution of mineral material within the soil profile and to the polycyclic nature of pedogenesis. Thus, the important damping role of soil lies in the sequestration of large amounts of biogenic carbon released in disturbed forest stands.

4. Conclusions

During the observation period, changes in species composition were revealed in all studied forest stands, along with a decrease in the proportion of fir trees as a consequence of pathological attrition caused by *P. proximus*. Depending on the severity of damage to the fir component of the forest by the alien bark beetle, inventory parameters such as density and completeness of the forest stands were diminished, even down to the appearance of open spaces.

The increase in the amount of deposited carbon in the pool of woody vegetation is due to a number of factors: radial growth of live trees, the emergence of undergrowth into the main layer, and the accumulation of substantial amounts of mortmass represented by dead standing trees that retain the sequestration function.

Disturbances caused by *P. proximus* led to an increase in the thickness of ground litter and to the concentration of biogenic elements in it (especially carbon and nitrogen). This tendency clearly manifests itself at the final point in the time-series of the observed successional changes. Meanwhile, there was an increase in the C/N ratio, due to intensified processes of transformation of mortmass, its mineralization and humification, partial transition of nitrogen into forms accessible to plants, and its entry into the biological cycles, or owing to the removal of N from the landscape. Therefore, in disturbed ecosystems, soil plays a major role in the sinking of biogenic C.

Due to the rapid rate of degradation of forest stands under the influence of *P. proximus*, a large number of dead standing and fallen trees accumulate in forest stands. Spikes of bark beetle abundance cause an appreciable transfer of carbon from the live carbon pool (stored in live trees) to the dead carbon pool, which is a source of future C emissions from heterotrophic decomposition and forest fires. Nonetheless, outbreaks of the pest are limited by the presence of a suitable food supply and favorable weather conditions.

Our study was not exhaustive regarding the effects of alien pest outbreaks on the carbon balance, as this work does not cover the entire diversity of soil-related and plant-related conditions of ecosystems affected by such a strong factor of zoogenic successions. Furthermore, effects on soil cover and undergrowth were not evaluated. Nevertheless, knowledge of the time course and patterns of re-distribution of carbon reserves is important, as a scientific basis for the management of forest stands disturbed by alien bark beetles. The dynamics of this adverse process and its cyclical nature will require further research.

Author Contributions: Conceptualization, I.A.K.; methodology, E.M.B., N.A.S., I.G.G., A.N.N. and D.A.K.; formal analysis, E.M.B., N.A.S., I.G.G., A.N.N. and D.A.K.; investigation, I.A.K., E.M.B., N.A.S., I.G.G., A.N.N. and D.A.K.; data curation, E.M.B., N.A.S., I.G.G., A.N.N. and D.A.K.; writing—original draft preparation, I.A.K., E.M.B., N.A.S., I.G.G., A.N.N. and D.A.K.; writing—review and editing, I.A.K.; visualization, E.M.B., N.A.S., I.G.G., A.N.N. and D.A.K.; supervision, I.A.K.; project administration, I.A.K.; funding acquisition, I.A.K. All authors have read and agreed to the published version of the manuscript.

Funding: The study was supported by Ministry of Science and Higher Education of the Russian Federation project No. FWRG-2022-0001.

Data Availability Statement: Raw data are available upon request.

Acknowledgments: The team of authors expresses sincere gratitude to employees of the Regional Committee for Natural Resources of Tomsk Oblast and in particular to E.Yu. Khrapov for logistic support of the field work. The authors are thankful to the Shared Research Facilities of the Tomsk Scientific Center of the Siberian Branch of the RAS for providing the DELTA V Advantage isotope mass spectrometer combined with a Flash 2000 elemental analyzer and to G.V. Simonova for carrying out the analyses.

Conflicts of Interest: The authors declare no conflicts of interest. The funders had no role in the design of the study; in the collection, analyses, or interpretation of the data; in the writing of the manuscript; or in the decision to publish the results.

Appendix A

Table A1. Scale of vitality categories of fir trees in the outbreak foci of *Polygraphus proximus* Blandf.

Tree Category	Crown Features	Trunk Features	Internal Features
I. Healthy, with no signs of weakening. Not attacked by *P. proximus.*	Crown is thick and expansive; needles are green and shiny.	Mechanical damage and streaks of resinosis are absent.	Bast is not damaged.

Table A1. *Cont.*

Tree Category	Crown Features	Trunk Features	Internal Features
II. Weakened. Attacked by *P. proximus* but the pest has not settled (unsuccessful attempts at colonization).	Crown may be similar to that of a healthy tree, with no signs of weakening, or it may be thinned, flag-like; several branches have needles colored bright red at the ends. There may be signs of fir broom rust (witches' brooms).	Moderate numbers of fresh and/or old streaks of resinosis on the trunk. Entrance holes of *P. proximus* are resin soaked (unsuccessful attempts at colonization). There may be signs of fir broom rust (possibly 1–3 cerous ulcers on the trunk, growths on the branches).	Bast is fresh, white, necrotic spots of various sizes in places of unsuccessful attempts at colonization by *P. proximus.*
III. Heavily weakened. Attacked by *P. proximus* but not colonized.	Crown, depending on the time and intensity of colonization, may be healthy but sparser, with pale-green needles, or more than half of the branches carry drying out needles. Witches' brooms are common.	Intense fresh and/or oldresin bleeding. In someplaces at the bottom of the trunk, there are entrance holes of *P. proximus*, which are not resin soaked. Signs of fir broom rust (numerous cancerous ulcers, growths on the branches) are common. Cracks on the trunk.	Bast is the same as in trees from category II. An entrance channel and nuptial chamber are resin soaked, failed attempts of colonization by *P. proximus.*
IV. Drying (dying). Colonized by *P. proximus.*	Needles in the upper part of the crown are still green; beneath, they have a bright red color.	Old streaks of resinosis may be seen. Numerous entrance holes without resinosis on the surface of bark.	Families of *P. proximus* under bark. Bast is mostly fresh, with necrotic spots near the nests of the bark beetles.
V. A recent dead tree.	Needles in the crown are completely dead, red, retained.	Exit holes of *P. proximus* can be seen on bark.	Different stages of *P. proximus* development under bark. Bast is moist, growing brown.
VI. A tree died in previous years (long-dead tree).	Crown is dead, gray. Needles fall off, down to their complete absence. Depending on the year of drying, branches of various orders fall off.	Numerous exit holes of *P. proximus* on bark. The bark is dry, easily comes off, and falls off when considerably damaged by insects.	Bast is brown and dry. Sap wood has tunnels of *P. proximus*, pupal chambers.

Appendix B

Table A2. The mean carbon concentration in various fractions of wood of the taxa under study.

The Genus of Trees	Fractional Part of Phytomass	Average Carbon Content, %	The Average Value of the Tree Species, %	Standard Error
Betula	Stem	46.9682	47.41	0.71
	Branches	50.11382		1.19
	Foliage	46.73186		0.79
	Root	45.83282		0.93
Picea	Stem	48.11803	48.85	0.2
	Branches	48.28587		0.23
	Foliage	47.4407		1.95
	Root	51.54453		0.47
Abies	Stem	46.76737	49.14	1.04
	Branches	48.8517		0.52
	Foliage	51.22855		2.02
	Root	49.7323		0.49
Pinus sibirica	Stem	50.6009	51.47	0.15
	Branches	53.45648		0.69
	Foliage	51.05883		0.7
	Root	50.7784		2.2
Populus tremula	Stem	48.9508	47.76	0.73
	Branches	48.66423		0.52
	Foliage	48.4591		1.13
	Root	44.9507		0.83
Pinus sylvestris	Stem	50.35818	48.76	0.66
	Branches	52.63315		0.05
	Foliage	42.5419		6.85
	Root	49.49117		0.61

References

1. Dixon, R.K.; Solomon, A.M.; Brown, S.; Houghton, R.A.; Trexier, M.C.; Wisniewski, J. Carbon pools and flux of global forest ecosystems. *Science* **1994**, *263*, 185–190. [CrossRef] [PubMed]
2. Gwynn-Jones, D.; Saugier, B.; Roy, J.; Mooney, H.A. Terrestrial global productivity. *Ann. Bot.* **2002**, *89*, 797–798. [CrossRef]
3. Houghton, R.A.; Nassikas, A.A. Negative emissions from stopping deforestation and forest degradation, globally. *Glob. Chang. Biol.* **2018**, *24*, 350–359. [CrossRef] [PubMed]
4. Hurteau, M.D.; North, M.P.; Koch, G.W.; Hungate, B.A. Managing for disturbance stabilizes forest carbon. *Proc. Natl. Acad. Sci. USA* **2019**, *116*, 10193–10195. [CrossRef] [PubMed]
5. Bazhina, E.V.; Tretyakova, I.N. Towards a problem of Fir decline. *Uspekhi Sovrem. Biologii.* **2001**, *121*, 626–631.
6. Bazhina, E.V.; Storozhev, V.P.; Tretyakova, I.N. Dieback of Fir-Siberian Stone pine forests under technogenic pollution in the Kuznetsky Alatau Mountains. *Lesovedenie* **2013**, *2*, 15–21.
7. Johnstone, J.F.; Chapin, F.S. Fire Interval Effects on Successional Trajectory in Boreal Forests of Northwest Canada. *Ecosystems* **2006**, *9*, 268–277. [CrossRef]
8. Allen, C.D.; Macalady, A.K.; Chenchouni, H.; Bachelet, D.; McDowell, N.; Vennetier, M.; Kitzberger, T.; Rigling, A.; Breshears, D.D.; Hogg, E.H.; et al. A global overview of drought and heat-induced tree mortality reveals emerging climate change risks for forests. *For. Ecol. Manag.* **2010**, *259*, 660–684. [CrossRef]
9. Groisman, P.; Bulygina, O.; Henebry, G.; Speranskaya, N.; Shiklomanov, A.; Chen, Y.; Tchebakova, N.; Parfenova, E.; Tilinina, N.; Zolina, O.; et al. Dryland belt of Northern Eurasia: Contemporary environmental changes and their consequences. *Environ. Res. Lett.* **2018**, *13*, 115008. [CrossRef]
10. Kharuk, V.I.; Im, S.T.; Petrov, I.A.; Dvinskaya, M.L.; Shushpanov, A.S.; Golyukov, A.S. Climate-driven conifer mortality in Siberia. *Glob. Ecol. Biogeogr.* **2020**, *30*, 543–556. [CrossRef]
11. Voronin, V.I.; Sofronov, A.P.; Morozova, T.I.; Oskolkov, V.A.; Sukhovol'skii, V.G.; Kovalev, A.V. The landscape-specific occurrence of bacterial diseases in dark-coniferous forests on Khamar-Daban range (Southern Cisbaikalia). *Geogr. Nat. Resour.* **2019**, *4*, 56–65.
12. Kirpotin, S.N.; Callaghan, T.V.; Peregon, A.M.; Babenko, A.S.; Berman, D.I.; Bulakhova, N.A.; Byzaakay, A.A.; Chernykh, T.M.; Chursin, V.; Interesova, E.A.; et al. Impacts of environmental change on biodiversity and vegetation dynamics in Siberia. *Ambio* **2021**, *50*, 1926–1952. [CrossRef] [PubMed]
13. Fei, S.; Phillips, J.; Shouse, M. Biogeomorphic impacts of invasive species. *Annu. Rev. Ecol. Evol. Syst.* **2014**, *45*, 69–87. [CrossRef]
14. Liebhold, A.M.; Brockerhoff, E.G.; Nunez, M.A. Biological invasions in forest ecosystems: A global problem requiring international and multidisciplinary integration. *Biol. Invasions* **2017**, *19*, 3073–3077. [CrossRef]
15. Seebens, H.; Blackburn, T.M.; Dyer, E.E.; Genovesi, P.; Hulme, P.E.; Jeschke, J.M.; Pagad, S.; Pyšek, P.; van Kleunen, M.; Winter, M.; et al. The global rise in emerging alien species results from increased accessibility of new source pools. *Proc. Natl. Acad. Sci. USA* **2018**, *115*, E2264–E2273. [CrossRef] [PubMed]
16. Musolin, D.L.; Kirichenko, N.I.; Karpun, N.N.; Mandelshtam, M.Y.; Selikhovkin, A.V.; Zhuravleva, E.N.; Aksenenko, E.V.; Golub, V.B.; Kerchev, I.A.; Vasaitis, R.; et al. Invasive pests of forests and urban trees in Russia: Origin pathways, damage, and management. *Forests* **2022**, *13*, 521. [CrossRef]
17. Krivets, S.A.; Kerchev, I.A.; Bisirova, E.M.; Demidko, D.A.; Pet'ko, V.M.; Baranchikov, Y.N. Distribution of the four-eyed fir bark beetle *Polygraphus proximus* Blandf. (Coleoptera, Curculionidae: Scolytinae) in Siberia. *Izvestia Sankt-Peterburgskoj Lesotehniceskoj Akademii* **2015**, *211*, 33–45. (In Russian)
18. Baranchikov, Y.N.; Krivets, S.A. About professional skills in determination of insects: How the occurrence of new aggressive invasive fir pest in Siberia was missed. *Ecol. South. Sib. Adjac. Territ.* **2010**, *14*, 50–52. (In Russian)
19. Bystrov, S.O.; Antonov, I.A. First record of the four-eyed beetle *Polygraphus proximus* Blandford, 1894 (Coleoptera: Curculionidae, Scolytinae) from Irkutsk Province, Russia. *Entomol. Rev.* **2019**, *98*, 54–55. [CrossRef]
20. Dedyukhin, S.V.; Titova, V.V. Finding of the bark beetle *Polygraphus proximus* Blandford, 1894 (Coleoptera, Curculionidae: Scolytinae) in Udmurtia. *Russ. J. Biol. Invasions* **2021**, *12*, 258–263. [CrossRef]
21. Kerchev, I.A. Ecology of four-eyed fir bark beetle *Polygraphus proximus* Blandford (Coleoptera: Curculionidae, Scolytinae) in the West Siberian region of invasion. *Russ. J. Biol. Invasions* **2014**, *5*, 176–185. [CrossRef]
22. Takagi, E.; Yamanaka, S. Reemergence and sister brood establishment in the bark beetle *Polygraphus proximus* (Coleoptera: Curculionidae: Scolytinae) under laboratory conditions. *Appl. Entomol. Zool.* **2024**, *59*, 1–6. [CrossRef]
23. Kerchev, I.A.; Bisirova, E.M.; Krivets, S.A. Effect of the Four-Eyed Fir Bark Beetle Invasion on the Species Composition and Structure of the Siberian Fir Stem Pest Complex. *Contemp. Probl. Ecol.* **2022**, *15*, 270–281. [CrossRef]
24. Pashenova, N.V.; Kononov, A.V.; Ustyantsev, K.V.; Blinov, A.G.; Pertsovaya, A.A.; Baranchikov, Y.N. Ophiostomatoid fungi associated with the four-eyed fir bark beetle on the territory of Russia. *Russ. J. Biol. Invasions* **2018**, *9*, 63–74. [CrossRef]
25. Krivets, S.A.; Bisirova, E.M.; Kerchev, I.A.; Pats, E.N.; Chernova, N.A. Transformation of taiga ecosystems in the Western Siberian invasion focus of four-eyed fir bark beetle *Polygraphus proximus* Blandford (Coleoptera: Curculionidae, Scolytinae). *Russ. J. Biol. Invasions* **2015**, *6*, 94–108. [CrossRef]
26. Demidko, D.A. The dates of invasion of four-eyed fir bark beetle *Polygraphus proximus* Blandford (Coleoptera: Curculionidae, Scolytinae) in Tomsk Oblast. *Izvestia Sankt-Peterburgskoj Lesotehniceskoj Akademii* **2014**, *207*, 225–234. (In Russian)
27. Alekseev, V.F. Diagnostics of tree vitality and stand condition. *Lesovedenie* **1989**, *4*, 51–57. (In Russian with English summary)

28. Lepekhin, A.A. Methods for determining the share of participation of a group of trees in forest pathological monitoring. *Lesnoye khozyaystvo* **2007**, *5*, 39–40. (In Russian)
29. Rumyancev, D.E.; Lipatkin, V.A.; Cherakshev, A.V.; Vorobyova, N.S. *Metodicheskie Rekomendacii po Otboru Kernov Drevesiny dlya celej Dendrohronologicheskih Issledovanij v Lesovedenii i Lesovodstve*; Professional'naya Nauka: Moscow, Russia, 2022; 44p. (In Russian) [CrossRef]
30. Usol'tsev, V.A.; Tsepordey, I.S.; Noritsin, D.V. Allometric models of single-tree biomass for forest-forming species of the Urals. *For. Russ. Econ. Them* **2022**, *1*, 4–14. [CrossRef]
31. Usol'tsev, V.A.; Chasovskikh, V.P.; Noritsina, Y.V.; Noritsin, D.V. Allometric models of tree biomass for airborne laser scanning and ground inventory of carbon pool in the forests of Eurasia: Comparative analysis. *Sibirskij Lesnoj Zurnal (Sib. J. For. Sci.)* **2016**, *4*, 68–76. [CrossRef]
32. Mukhortova, L.V.; Sergeeva, O.V.; Demidko, D.A.; Krivobokov, L.V.; Baranchikov, Y.N. Dynamics of coarse woody debris stocks in the fir forests damaged by the bark beetle *Polygraphus proximus* Blandf. (Coleoptera: Curculionidae, Scolytinae). Dendrobiont invertebrates and fungi and their role in forest ecosystems (XI Readings in memory of O.A. Kataev). In *Proceedings of the All-Russian Conference with International Participation, St. Petersburg, Russia, 24–27 November 2020*; Musolin, D.L., Kirichenko, N.I., Selikhovkin, A.V., Eds.; St. Petersburg State Forestry University Named after S.M. Kirova: St. Petersburg, Russia, 2020; pp. 231–232. (In Russian)
33. Isaeva, L.N. Physical properties of wood of growing trees at different stages of decay. In *Wood and Wood Materials*; V.N. Sukachev Institute of Forest SB RAS: Krasnoyarsk, Russia, 1974; pp. 28–39. (In Russian)
34. Shorokhova, E.V.; Shorokhov, A.A. *Characteristics of Detritus Decay Classes for Spruce, Birch, and Aspen in Middle Taiga Spruce Forests*; St. Petersburg Forestry Research Institute Publishers: St. Petersburg, Russia, 1999; Volume 1, pp. 17–23.
35. Shein, E.V.; Karpachevskii, L.O. (Eds.) *Theories and Methods of Soil Physics*; Grif and K: Moscow, Russian, 2007; p. 616.
36. Pansu, M.; Gautheyrou, J. *Handbook of Soil Analysis: Mineralogical, Organic and Inorganic Methods*, 1st ed.; Springer: Heidelberg, Germany, 2007; 993p.
37. Lebedev, A.T. *Mass Spectrometry for the Analysis of the Environment*; Tekhnosfer Publ.: Moscow, Russia, 2013; p. 632.
38. *APPLICATION NOTE E-EMA-001-2021/A2*; CHNS Determination in Reference Soil Samples; VELP Scientifica: Usmate Velate, Italy, 2021; 3p.
39. Takagi, E.; Köbayashi, K.; Takei, S.Y.; Masaki, D. Trunk diameter influences attack by Polygraphus proximus and subsequent mortality of Abies veitchii. *For. Ecol. Manag.* **2021**, *479*, 118617. [CrossRef]
40. Wermelinger, B. Development and distribution of predators and parasitoids during two consecutive years of an *Ips typographus* (Col., Scolytidae) infestation. *J. Appl. Ent.* **2002**, *126*, 521–527. [CrossRef]
41. *Good Practice Guidelines for Land Use, Land-Use Change and Forestry*; IPCC National Greenhouse Gas Inventories Programme; IPCC, WMO: Moscow, Russia, 2003; 330p.
42. Lamlom, S.; Savidge, R. A reassessment of carbon content in wood: Variation within and between 41 North American species. *Biomass Bioenergy* **2003**, *25*, 381–388. [CrossRef]
43. Kerchev, I.A.; Krivets, S.A.; Mandelshtam, M.Y.; Ilinsky, Y.Y. Small Spruce Bark Beetle *Ips amitinus* (Eichhoff, 1872) (Coleoptera, Curculionidae: Scolytinae): A New Alien Species in West Siberia. *Entomol. Rev.* **2019**, *99*, 639–644. [CrossRef]
44. Ellison, A.M.; Orwig, D.A.; Fitzpatrick, M.C.; Preisser, E.L. The Past, Present, and Future of the Hemlock Woolly Adelgid (*Adelges tsugae*) and Its Ecological Interactions with Eastern Hemlock (*Tsuga canadensis*) Forests. *Insects* **2018**, *9*, 172. [CrossRef] [PubMed]
45. Hobbie, E.A.; Rinne-Garmston (Rinne), K.T.; Penttilä, R.; Vadeboncoeur, M.A.; Chen, J.; Mäkipää, R. Carbon and nitrogen acquisition strategies by wood decay fungi influence their isotopic signatures in *Picea abies* forests. *Fungal Ecol.* **2021**, *52*, 101069. [CrossRef]
46. Bégin, C.; Gingras, M.; Savard, M.M.; Marion, J.; Nicault, A.; Bégin, Y. Assessing tree-ring carbon and oxygen stable isotopes for climate reconstruction in the Canadian northeastern boreal forest. *Palaeogeogr. Palaeoclimatol. Palaeoecol.* **2015**, *423*, 91–101. [CrossRef]
47. *Program of Emergency Measures for Biological Control of Insect Pests in the Forests of the Krasnoyarsk Territory*; Report on the World Bank Project Loan 3806-RU; Moscow, Russia, 1997; 151p.
48. Klutsch, J.G.; Negrón, J.F.; Costello, S.L.; Rhoades, C.C.; West, D.R.; Popp, J.; Caissie, R. Stand characteristics and downed woody debris accumulations associated with a mountain pine beetle (*Dendroctonus ponderosae* Hopkins) outbreak in Colorado. *For. Ecol. Manage.* **2009**, *258*, 641–649. [CrossRef]
49. Fei, S.; Morin, R.S.; Oswalt, C.M.; Liebhold, A.M. Biomass losses resulting from insect and disease invasions in US forests. *Proc. Natl. Acad. Sci. USA* **2019**, *116*, 17371–17376. [CrossRef]
50. Shvidenko, A.Z.; Schepaschenko, D.; Nilsson, S. Assessment of woody detritus in forests of Russia. *For. Surv. For. Manag.* **2009**, *1*, 133–147. (In Russian)
51. Klimchenko, A.V.; Verkhovets, S.V.; Slinkina, O.A.; Koshurnikova, N.N. Stocks of large woody remains in the middle taiga ecosystems of the Yenisei Siberia. *Geogr. Nat. Resour.* **2011**, *2*, 91–97. (In Russian)
52. Cobb, R.C.; Orwig, D.A.; Currie, S. Decomposition of green foliage in eastern hemlock forests of southern New England impacted by hemlock woolly adelgid infestations. *Can. J. For. Res.* **2006**, *36*, 1331–1341. [CrossRef]
53. Knoepp, J.D.; Vose, J.M.; Clinton, B.D.; Hunter, M.D. Hemlock infestation and mortality: Impacts on nutrient pools and cycling in Appalachian forests. *Soil Sci. Soc. Am. J.* **2011**, *75*, 1935–1945. [CrossRef]

54. Yorks, T.E.; Leopold, D.J.; Raynal, D.J. Effects of Tsuga canadensis mortality on soil water chemistry and understory vegetation: Possible consequences of an invasive insect herbivore. *Can. J. For. Res.* **2003**, *33*, 1525–1537. [CrossRef]
55. Nuckolls, A.E.; Wurzburger, N.; Ford, C.R.; Hendrick, R.L.; Vose, J.M.; Kloeppel, B.D. Hemlock Declines Rapidly with Hemlock Woolly Adelgid Infestation: Impacts on the Carbon Cycle of Southern Appalachian Forests. *Ecosystems* **2009**, *12*, 179–190. [CrossRef]